Wilson, P.A., Lyle, M., Janecek, T.R., and Firth, J.V. (Eds.)
Proceedings of the Ocean Drilling Program, Scientific Results Volume 199

12. DATA REPORT: CORRECTION OF CORE PHYSICAL PROPERTIES AND COMPOSITE DEPTHS FOR SITES 1215–1222 USING CORE-LOG CORRELATION–DERIVED REBOUND COEFFICIENTS[1]

B.R. Rea[2] and P. Gaillot[3,4]

ABSTRACT

A methodology was developed that can be used to derive rebound coefficients for the correction of rebounded core physical properties (density, porosity, and void ratio) and spliced meters composite depths (mcds) to in situ values. The increasing-with-depth mismatch between logging depths (density curves were used in this instance) and mcd depths are treated as consolidation tests, only somewhat larger. Core physical properties and mcd depths are first corrected for hydraulic rebound (here almost 4 m of offset at 190 meters below seafloor [mbsf]); the remaining offset is attributed to mechanical (porosity) rebound. The offset between the hydraulic rebound–corrected depths and logging depths are used in conjunction with hydraulic rebound–corrected discrete core sample physical properties to obtain rebound coefficients (C_r values) for the nannofossil and radiolarian oozes at Ocean Drilling Program (ODP) Sites 1218 and 1219. Using the nannofossil ooze rebound coefficients, the Site 1218 mcds are corrected upcore from a tie point at 80 mbsf, allowing derivation of a linear compression for the overlying pelagic clay unit. The three relationships derived from these two sites can then be used to correct the core physical properties and mcds for the other sites cored during ODP Leg 199. The corrected Site 1219 spliced density curve is presented as an example of this process. This method can also be applied to other ODP and Deep Sea Drilling

[1]Rea, B.R., and Gaillot, P., 2004. Data report: Correction of core physical properties and composite depths for Sites 1215–1222 using core-log correlation–derived rebound coefficients. *In* Wilson, P.A., Lyle, M., Janecek, T.R., and Firth, J.V. (Eds.), *Proc. ODP, Sci. Results*, 199, 1–21 [Online]. Available from World Wide Web: <http://www-odp.tamu.edu/publications/199_SR/VOLUME/CHAPTERS/208.PDF>. [Cited YYYY-MM-DD]

[2]Department of Geography and Environment, University of Aberdeen, Elphinstone Road, Aberdeen, Scotland AB24 3UF, United Kingdom.
b.rea@abdn.ac.uk
[3]Imagerie Géophysique FRE 2639, Université Pau et des Pays de l'Adour, Avenue de l'Université, BP 576, 64012 Pau Cedex, France.
[4]LGHF, ISTEEM, Université Montpellier II, Place Eugène Bataillon, 34095 Montpellier Cedex, France.

Initial receipt: 15 April 2004
Acceptance: 27 July 2004
Web publication: 9 November 2004
Ms 199SR-208

Project sites where unlithified pelagic sediments were cored, a stratigraphic splice can be/has been constructed, and downhole logging was undertaken. Using this approach, it may be possible to produce locally to regionally applicable rebound-correction relationships for a number of pelagic sediments.

INTRODUCTION

The stratigraphic splices composed during Leg 199, through the unlithified sediments, exhibit the well-known increasing-with-depth offset from true meters below seafloor (mbsf) depth. This offset is the result of some combination of the following: hydraulic rebound (due to pore water expansion), mechanical (porosity) rebound, and erroneous additions to the splice. The first two processes impact the core physical properties, resulting in a decrease in density and velocity with a concomitant increase in porosity. All of these processes combined result in the meters composite depth (mcd) scale becoming increasingly offset from the true (mbsf) depth (Fig. **F1**). The magnitude of physical properties and the associated mcd offset are typically corrected either using published depth rebound functions (e.g., Hamilton, 1976), or using results from consolidation tests undertaken on whole-round samples (e.g., MacKillop et al., 1995; Moran, 1997; MacKillop, 2000). In the absence of downhole logs (which are assumed to be correct in depth and magnitude) or for the nonlogged formation above the pipe, core physical properties and composite splices are critical for computing synthetic seismograms (calculated from in situ sediment density and velocity [e.g., Mayer et al., 1985, 1986]), thus tying point-source depth-domain core and logging data to time-domain seismic data. As no whole rounds were taken for consolidation testing during Leg 199, the methodology presented here was developed and utilizes spliced core to logging depth mismatches to compute rebound coefficients (C_r) (see Table **T1** for a list of symbols and subscripts). This procedure can only be undertaken where there is a good core splice and wireline logging data are available, and it makes the assumption that the sediments are not overconsolidated. The results are, circumstances permitting, applicable to core sections above the pipe (where logging data are unavailable) and to holes/sites where logging has not been undertaken.

F1. Multiple hole density data, p. 11.

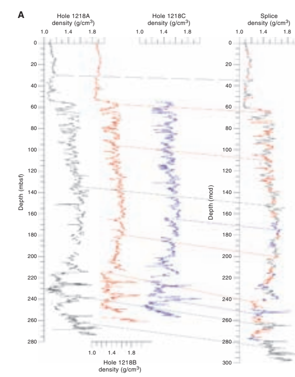

T1. List of symbols, p. 18.

A C_r relationship is derived for nannofossil ooze from Site 1218, where a continuous sediment section was constructed (Shipboard Scientific Party, 2002a) and advanced piston coring (APC) cores were recovered down to ~190 mbsf. Downhole logging was undertaken in Hole 1218A with the pipe set at 80 mbsf, thus providing 110 m of overlap between the logging and the core splice (80–190 mbsf). The C_r relationship for radiolarian ooze (150.8–225 mbsf) was derived from Site 1219, where APC cores were recovered to 225 mbsf and logging data were available through the same interval (Shipboard Scientific Party, 2002c). In addition to this, a linear compression relationship for the ubiquitous upper clay lithofacies was derived from Site 1218.

METHODOLOGY

A brief description of the methodology applied in this process is presented here with full details provided in Rea and Gaillot (submitted [**N1**]). The following describes the procedure undertaken for the nannofossil ooze at Site 1218. Density data from both passes of the Hostile Environment Litho-Density Tool (HLDT) were quality controlled, depth matched, and stacked. The core splice density curve was depth matched to the stacked logging density curve (Fig. **F1B**) using the core-log integration software program Sagan (**www.ldeo.columbia.edu/BRG/ODP/ODP/CLIP/download.html**), which provides output in drillers (mbsf), core-splice (mcd), and logging depth-matched (meters equivalent log depth [meld]) depths. No obvious erroneous additions to the mcd splice were found. The core-log depth match was undertaken three times, using increasing numbers of tie points, to check consistency. The depth matches showed good repeatability, and the number of tie points was found to be insignificant on subsequent calculations.

Gamma ray attenuation (GRA) density was corrected to the discrete sample (moisture and density [MAD]) density, and these corrected GRA_c data are significantly closer to the logging densities, though the GRA densities are still lower than the logging densities.

Nannofossil Ooze

Hydraulic Rebound

Pressure differences between in situ conditions and those at the sea surface result in hydraulic rebound of the pore water, manifest as a reduction in water density (e.g., 1.024 g/cm^3 laboratory measured → 1.049 g/cm^3 at 100 mbsf in Hole 1218A, where the water depth was 4828 m) that concomitantly increases the pore water volume and thus the sediment porosity. Given the significant water depths at sites used in this study (4800–5000 m) it is prudent to correct the sediment density/porosity for hydraulic rebound. Full details of the procedure are given in Rea and Gaillot (submitted [**N1**]), and Table **T2** presents the values used for in situ density in all subsequent corrections. A cross-plot of GRA_{hc} (MAD and hydraulic rebound–corrected GRA density) and the in situ recorded logging data show that the core data plot close to the 1:1 line (Fig. **F2**). Correcting for hydraulic rebound results in compression of the mcds by 3.69 m at a depth of 190 mbsf, which still leaves a depth mismatch of just under 21 m between the logging and the hydraulic rebound–corrected depths (mcd_{hc}). This remaining depth offset is assumed to be the result of mechanical rebound (porosity rebound) of the unlithified sediments.

T2. In situ water density, p. 19.

F2. Logging and corrected GRA_{hc} densities, p. 13.

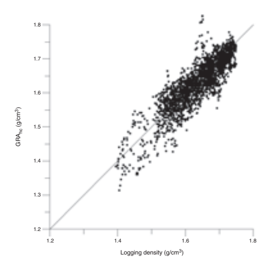

Mechanical/Porosity Rebound

Mechanical rebound is manifest as an increase in void ratio (*e*) and porosity (ϕ) and a decrease in density (ρ) and sonic velocity (*v*). The core is confined laterally by the liner, so rebound is limited to one dimension (i.e., length). Thus, unloading and expansion of the recovered core is equivalent to a one-dimensional consolidation test (Fig. **F3**), details of which can be found in any soil mechanics text:

$$\Delta e = \log P'_i C_r, \tag{1}$$

where

e = e_{hc} (MAD and hydraulic rebound–corrected void ratio) – e_i (in situ void ratio),
P'_i = the effective in situ pressure, and
C_r = the rebound coefficient.

F3. Stress vs. void ratio for unlithified sediments, p. 14.

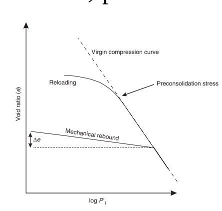

When constructing a spliced stratigraphic section (the norm during Ocean Drilling Program [ODP] paleoceanography legs), mechanical rebound results in an increasing-with-depth offset ΔL between the core (mcd) depth and the true (mbsf) depth (e.g., Ruddiman et al., 1987; Hagelberg et al., 1992, 1995). ΔL is determined from the difference between the (mcd_{hc}) depth and the logging (mbsf) depth. Two series of ΔL values are calculated for depth steps of 2 and 5 m downcore and can be used to calculate Δe:

$$\Delta L = (\Delta e)(L_{hc} - \phi_{hc} L_{hc}), \tag{2}$$

where

L_{hc} = the hydraulic rebound–corrected length (mcd_{hc}) and
ϕ_{hc} = the MAD and hydraulic rebound–corrected porosity (averaged over the depth step).

P'_i is calculated from the submerged unit weight (buoyant weight) using equation 3 (this assumes hydrostatic pore water pressures, a reasonable assumption given the sedimentation rates and age).

$$P'_i = (GRA_{hc} - \rho_{wi}) h_{hc}, \tag{3}$$

where

ρ_{wi} = the in situ pore water density (1.049 g/cm^3) and
h_{hc} = the hydraulic rebound–corrected depth step length (mcd_{hc}).

P'_i is calculated for each density data point, added to the total P'_i from above, and an average is calculated for the depth interval. Thus, P'_i and Δe calculated from equations 2 and 3 are used to calculate the C_r values using equation 1 for successive depth intervals (of 2 and 5 m) from 80 to 190 mbsf.

C_r values are obtained for the nannofossil ooze from 80 to 190 mbsf. For core correction the best correlation was obtained by cross-plotting C_r values against e_{hc} for the 5-m depth steps (Fig. **F4**), which yielded the following relationship:

F4. Void ratio vs. rebound coefficient, p. 15.

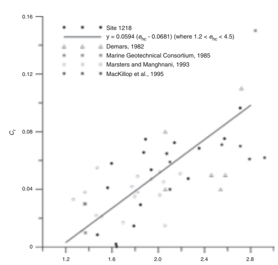

$$C_r = e_{hc} 0.0594 - 0.0681. \tag{4}$$

All depth intervals recording a decrease in the mcd-mbsf offset were excluded from the calculation and Figure **F4.** Equation 4 is invalid for void ratios outside of the range 1.2–4.5; in the core compression, any points lying outside this range are assigned C_r values of 0.09 and 0.2, respectively.

The Site 1218 hydraulic rebound–corrected core splice density curve was depth shifted by assigning C_r values using equation 4 (mcd_{fc}), and in situ density was calculated from equation 5 (GRA_{fc}).

$$GRA_{fc} = \phi_{fc} \rho_{iw} + (1 - \phi_{fc}) \rho_g, \tag{5}$$

where

ρ_g = grain density,
ρ_{iw} = in situ porewater density, and
ϕ_{fc} = final corrected (in situ) porosity: $\phi_{fc} = (e_{hc} - \Delta e)/[1 + (e_{hc} - \Delta e)]$.

The GRA_{fc}-mcd_{fc} (final corrected core splice density) curve (80–190 mbsf) is plotted along with the stacked logging curve in Figure **F5A,** with inset plots showing depth offset (meld – mcd_{fc}) vs. mbsf (Fig. **F5B**) and logging density vs. GRA_{fc} (Fig. **F5C**). The depth correction is accurate (Fig. **F5A**), with the offset between the corrected core splice (mbsf) and the logging depth–matched core splice (meld) being less than ±1 m for ~80% of the section (Fig. **F5B**); the greatest difference was 1.8 m. However, the corrected core splice density is greater (average = 0.045 g/cm^3) than the logging density, which is highlighted in the cross-plot (Fig. **F5C**). Consolidation test–derived C_r values from similar nannofossil oozes from a number of studies are also plotted on Figure **F4.** Clearly, the relationship obtained in this study agrees well with compression test–derived results. The apparent overcorrection of the density values suggests that there is an error either in the core density and the subsequent correction or the logging data. HLDT measurements are adversely affected by poor borehole conditions (e.g., washouts and wall roughness [e.g., Rider, 1996]), and in Hole 1218A the borehole was beyond the caliper range (18 in) and rough, especially between 95 and 130 mbsf. The magnitude of the HLDT measurements was verified by deriving a density log from the Phasor Dual Induction–Spherically Focused Resistivity Tool (DITE) log and core grain densities (Rea and Gaillot, submitted [**N1**]). The DITE-derived density curve represents a minimum for formation density and indicates that the HLDT measurements were affected by borehole washout, adding confidence to the corrected core density curve shown in Figure **F5A.**

F5. Corrected core densities and depth offsets, p. 16.

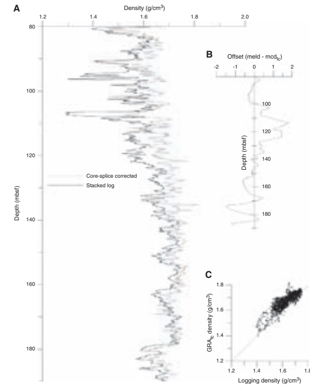

Radiolarian Ooze

The same methodology was applied to middle to late Eocene radiolarian ooze (150.8–225 mbsf) at Site 1219, where APC cores were recovered to 225 mbsf (Shipboard Scientific Party, 2002c). The quality of the core splice made the core-log matching somewhat more difficult than at Site 1218, and ultimately only five good rebound coefficients were derived. The best correlation with the C_r values was found with the percentage clay content (cl) (derived from light absorption spectroscopy [LAS] [Vanden Berg and Jarrad, 2002]), and the following power law expression (applicable to a lower limit of 27% clay) was used to assign rebound coefficients (a less well correlated relationship was also obtained for e_{hc}: $C_r = e_{hc}0.051 + 0.2613$):

$$C_r = 2.10^7 \text{ cl}^{-5.66}. \tag{6}$$

Pelagic Clay

At Site 1218, the nannofossil ooze core splice was corrected upward from the core-log tie point at 80 mbsf. This correction placed the top of the nannofossil ooze at ~51.32 mbsf (57.66 mcd_{hc}), which provided a linear compression value of 0.8901 for correcting the splice mcd_{hc} to true mbsf. Applying a linear correction to the clay interval is appropriate, as previous research has suggested that the mechanical rebound response of pelagic clays is linear to depths considerably in excess of 100 mbsf (Hamilton, 1976).

Site 1219

Figure **F6** presents, as an example of the procedure undertaken for all the sites, the corrected GRA_{fc}-mcd_{fc} (density) curve from Site 1219 is plotted along with the stacked HLDT logging density curve. The core depths have not been tied to the log, and in the lower part of the hole, especially in the radiolarian ooze, core breaks have not been accounted for in the splice. The depth correction to the radiolarian ooze is accurate (when individual sections are compared to the log); core breaks are the major cause of the depth mismatch (Fig. **F6A**). The magnitude of the density correction is good through most of the nannofossil and radiolarian oozes (Fig. **F6B**).

F6. GRA depth matches, p. 17.

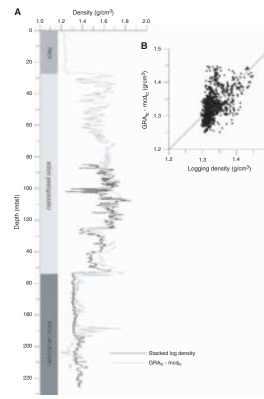

CORRECTED DATA

Corrections have been undertaken for each of the sites drilled during Leg 199 and include the spliced section for each individual hole. Data files are supplied as tab-delimited ASCII files (see the **"Supplementary Material"** contents list).

Splice

The splice is treated as a single continuous section, and any short data gaps have, where possible, been compressed assuming characteristics of the sediments immediately above. This may over- or under-compress the gap, but the compression is valid again in the next section, which can, if desired, be repositioned to its cored mbsf depth and the mcd_{fc} depths shifted by addition or subtraction. Once the splice is unconstrained and is composed of appended sections, they have, where reasonable, been compressed in a similar fashion. This procedure was undertaken as far as possible, until the drillers mbsf and mcd_{fc} depths became too disparate. Table **T3** provides brief details on the depths to which the splice and appended sections are deemed acceptable.

T3. Validity of splice depth corrections to true in situ depths, p. 20.

Holes

The individual hole corrections have been undertaken using the same approach (as for the splice above) except that at the top of each core the depth is reset to the drillers depth in mbsf. This results in a mismatch between the base and top of consecutive cores. The length compressions are correct for each core, and the mcd_{fc} depths for each core length may be shifted to fit with cores above or below, as desired. As with the splice, areas of poor core data or short core gaps have been corrected by assuming characteristics of the sediments immediately above.

Data Files

Each corrected data set provides the following information:

Original drillers mbsf depths;
Depths corrected for hydraulic rebound and drilling disturbance (to MAD discrete sample values) depths (mcd_{hc}) and magnitudes, GRA_{hc} – density, ϕ_{hc} – porosity, and e_{hc} – void ratio; and

Final corrected (mechanical and hydraulic rebound and drilling disturbance) depths (mcd_{fc}) and magnitudes, GRA_{fc} – density, ϕ_{fc} – porosity, and e_{fc} – void ratio.

DISCUSSION

Composite depth scales and synthetic seismograms derived from core data are all erroneous until depths and physical property measurements have been corrected for coring disturbance and recovery-related rebound. Depth corrections can be made using published data (e.g., Hamilton, 1976), which proved unsatisfactory in this case, or by consolidation testing the cored sediments, which was not undertaken during Leg 199. The method developed here is, in effect, a consolidation test but removes the necessity for taking core whole-round samples. It does, however, require that downhole logs are available in at least one hole at one site. Problems associated with laboratory testing of samples, for example, sample size and quality, backpressuring issues, or bedding of the testing rig during loading (Fabricius, 2000) are removed.

Rebound coefficients derived using this method can, as with consolidation tests, be used for correction of core data in other holes in the same location and for sediments above the pipe, if circumstances permit (as in this study). By removing the need for core samples, this technique provides the opportunity to "revisit" sites cored and logged during Deep Sea Drilling Project and early legs of ODP. This methodology provides a useful tool to investigate the rebound characteristics of pelagic sediments from a range of deep marine environments and may be especially useful for assessing rebound through critical intervals/lithologies where is it difficult to get permission for whole-round core sampling.

CONCLUSIONS

A methodology has been presented to derive rebound coefficients to correct core physical properties and mcd depth scales back to in situ values. It does not require whole-round samples to be taken for consolidation testing; rather, it utilizes the increasing-with-depth offset between the core mcd and logging mbsf depth scales (Shipboard Scientific Party, 2002b) as a large-scale compression test. The only requirements are a continuous sedimentary splice (can be unconstrained in depth space provided it can still be depth matched to the downhole logs) and in situ acquired downhole logs.

Rebound coefficients (C_r) for nannofossil and radiolarian ooze and a linear compression for pelagic clays were obtained and used to correct the mcd depths and core physical properties above the pipe and for the non-logged sites. The methodology is applicable to the investigation of rebound relationships using only information available from the ODP Janus Web database (**www-odp.tamu.edu/database/**) (i.e., no core whole rounds are required).

ACKNOWLEDGMENTS

This research used data provided by the Ocean Drilling Program (ODP). ODP is sponsored by the U.S. National Science Foundation

(NSF) and participating countries under management of Joint Oceanographic Institutions (JOI). Thanks to the Leg 199 shipboard scientific party, Kerry Swain, and technicians on the rig floor of the *JOIDES Resolution*. Schlumberger/Geoquest supplied the log interpretation software Geoframe used for some of the work reported here.

REFERENCES

Demars, K.R., 1982. Unique engineering properties and compression behavior of deep-sea calcareous sediments. *In* Demars, K.R., and Chaney, R.C. (Eds.), *Geotechnical Properties, Behavior, and Performance of Calcareous Soils.* ASTM Spec. Tech. Publ., 777:97–112.

Fabricius, I.L., 2000. Interpretation of burial history and rebound from loading experiments and occurrence of microstylolites in mixed sediments of Caribbean sites 999 and 1001. *In* Leckie, R.M., Sigurdsson, H., Acton, G.D., and Draper, G. (Eds.), *Proc. ODP, Sci. Results,* 165: College Station, TX (Ocean Drilling Program), 177–190.

Hagelberg, T., Shackleton, N., Pisias, N., and Shipboard Scientific Party, 1992. Development of composite depth sections for Sites 844 through 854. *In* Mayer, L., Pisias, N., Janecek, T., et al., *Proc. ODP, Init. Repts.*, 138 (Pt. 1): College Station, TX (Ocean Drilling Program), 79–85.

Hagelberg, T.K., Pisias, N.G., Shackleton, N.J., Mix, A.C., and Harris, S., 1995. Refinement of a high-resolution, continuous sedimentary section for studying equatorial Pacific Ocean paleoceanography, Leg 138. *In* Pisias, N.G., Mayer, L.A., Janecek, T.R., Palmer-Julson, A., and van Andel, T.H. (Eds.), *Proc. ODP, Sci Results,* 138: College Station, TX (Ocean Drilling Program), 31–46.

Hamilton, E.L., 1976. Variations of density and porosity with depth in deep-sea sediments. *J. Sediment. Petrol.,* 46:280–300.

Marine Geotechnical Consortium, 1985. Geotechnical properties of northwest Pacific pelagic clays: Deep Sea Drilling Project Leg 86, Hole 576A. *In* Heath, G.R., Burckle, L.H., et al., *Init. Repts. DSDP,* 86: Washington (U.S. Govt. Printing Office), 723–758.

MacKillop, A.K., Moran, K., Jarrett, K., Farrell, J., and Murray, D., 1995. Consolidation properties of equatorial Pacific Ocean sediments and their relationship to stress history and offsets in the Leg 138 composite depth sections. *In* Pisias, N.G., Mayer, L.A., Janecek, T.R., Palmer-Julson, A., and van Andel, T.H. (Eds.), *Proc. ODP, Sci. Results,* 138: College Station, TX (Ocean Drilling Program), 357–369.

MacKillop, K., 2000. *Data report:* Correction of index properties and the meters composite depth scale using elastic properties of Leg 167 sediments. *In* Lyle, M., Koizumi, I., Richter, C., and Moore, T.C. (Eds.), *Proc. ODP, Sci. Results,* 167: College Station, TX (Ocean Drilling Program), 333–338.

Marsters, J.C., and Manghnani, M.H., 1993. Consolidation test results and porosity rebound of Ontong Java Plateau sediments. *In* Berger, W.H., Kroenke, L.W., Mayer, L.A., et al., *Proc. ODP, Sci. Results,* 130: College Station, TX (Ocean Drilling Program), 687–694.

Mayer, L.A., Shipley, T.H., Theyer, F., Wilkens, R.H., and Winterer, E.L., 1985. Seismic modeling and paleoceanography at Deep Sea Drilling Project Site 574. *In* Mayer, L., Theyer, F., Thomas, E., et al., *Init. Repts. DSDP,* 85: Washington (U.S. Govt. Printing Office), 947–970.

Mayer, L.A., Shipley, T.H., and Winterer, E.L., 1986. Equatorial Pacific seismic reflectors as indicators of global oceanographic events. *Science,* 233:761–764.

Moran, K., 1997. Elastic property corrections applied to Leg 154 sediment, Ceara Rise. *In* Shackleton, N.J., Curry, W.B., Richter, C., and Bralower, T.J. (Eds.), *Proc. ODP, Sci. Results,* 154: College Station, TX (Ocean Drilling Program), 151–155.

Rider, M.H., 1996. *The Geological Interpretation of Well Logs* (2nd ed.): Caithness (Whittles Publishing).

Ruddiman, W.F., Cameron, D., and Clement, B.M., 1987. Sediment disturbance and correlation of offset holes drilled with the hydraulic piston corer: Leg 94. *In* Ruddiman, W.F., Kidd, R.B., Thomas, E., et al., *Init. Repts. DSDP,* 94 (Pt. 2): Washington (U.S. Govt. Printing Office), 615–634.

Shipboard Scientific Party, 2002a. Explanatory notes. *In* Lyle, M., Wilson, P.A., Janecek, T.R., et al., *Proc. ODP, Init. Repts.*, 199 [Online]. Available from World Wide

Web: <http://www-odp.tamu.edu/publications/199_IR/chap_02/chap_02.htm>. [Cited 2003-05-19]

Shipboard Scientific Party, 2002b. Site 1218. *In* Lyle, M., Wilson, P.A., Janecek, T.R., et al., *Proc. ODP, Init. Repts.,* 199 [Online]. Available from World Wide Web: <http://www-odp.tamu.edu/publications/199_IR/chap_11/chap_11.htm>. [Cited 2003-05-19]

Shipboard Scientific Party, 2002c. Site 1219. *In* Lyle, M., Wilson, P.A., Janecek, T.R., et al., *Proc. ODP, Init. Repts.,* 199 [Online]. Available from World Wide Web: <http://www-odp.tamu.edu/publications/199_IR/chap_12/chap_12.htm>. [Cited 2003-09-15]

Vanden Berg, M.D., and Jarrad, R.D., 2002. Determination of equatorial Pacific mineralogy. *In* Lyle, M., Wilson, P.A., Janecek, T.R., et al., *Proc. ODP, Init. Repts.,* 199 [Online]. Available from World Wide Web: <http://www-odp.tamu.edu/publications/199_IR/chap_05/chap_05.htm>. [Cited 2003-09-18]

Figure F1. A. Multiple hole density data from Site 1218 spliced into a composite density profile plotted in an expanded meters composite depth framework (Shipboard Scientific Party, 2002a). (Continued on next page.)

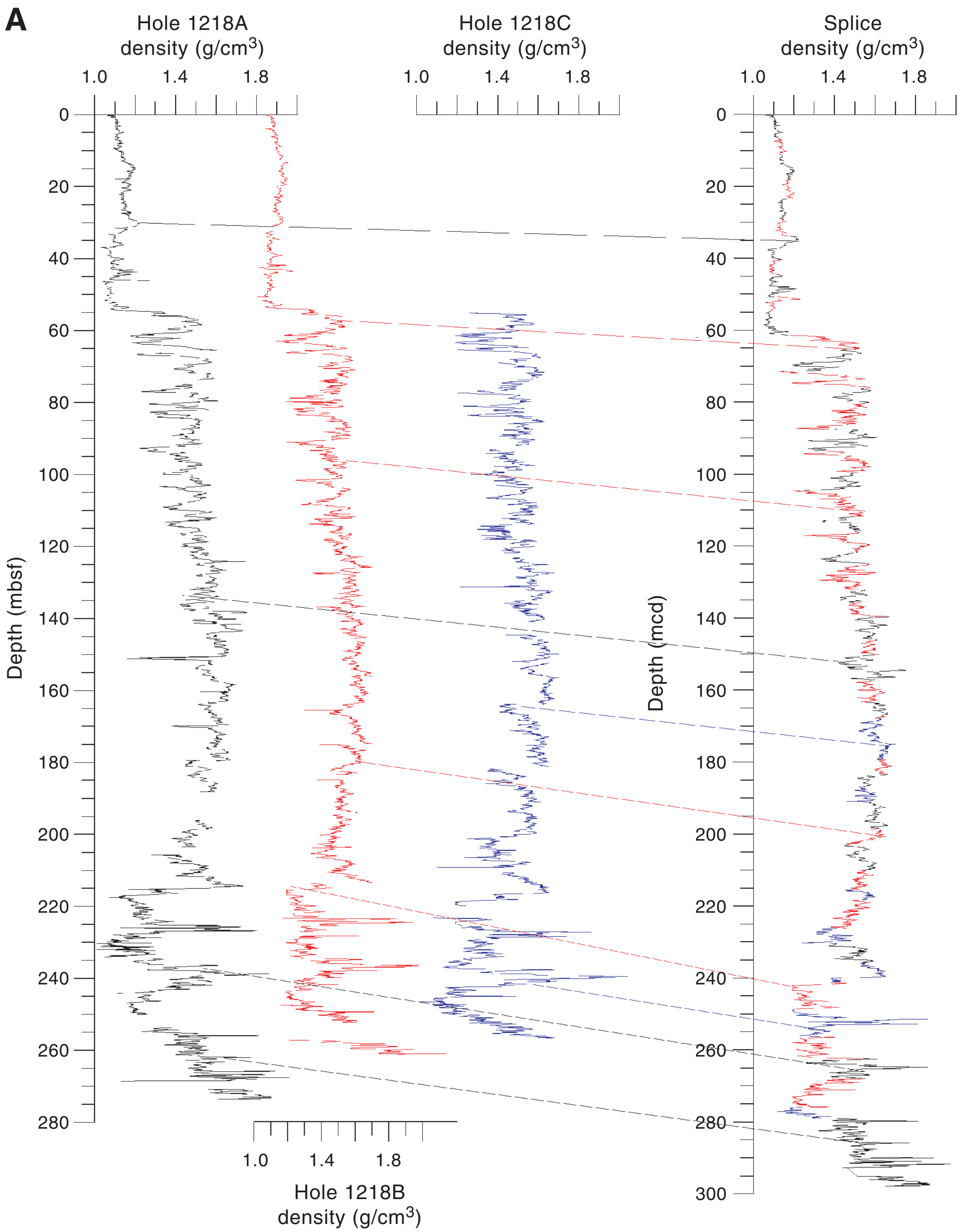

Figure F1 (continued). B. Cross-plot of the in situ acquired logging density and the rebound core density. The solid line is 1:1. **C.** Depth-matched core splice and stacked logging density curves plotted in (logging) mbsf.

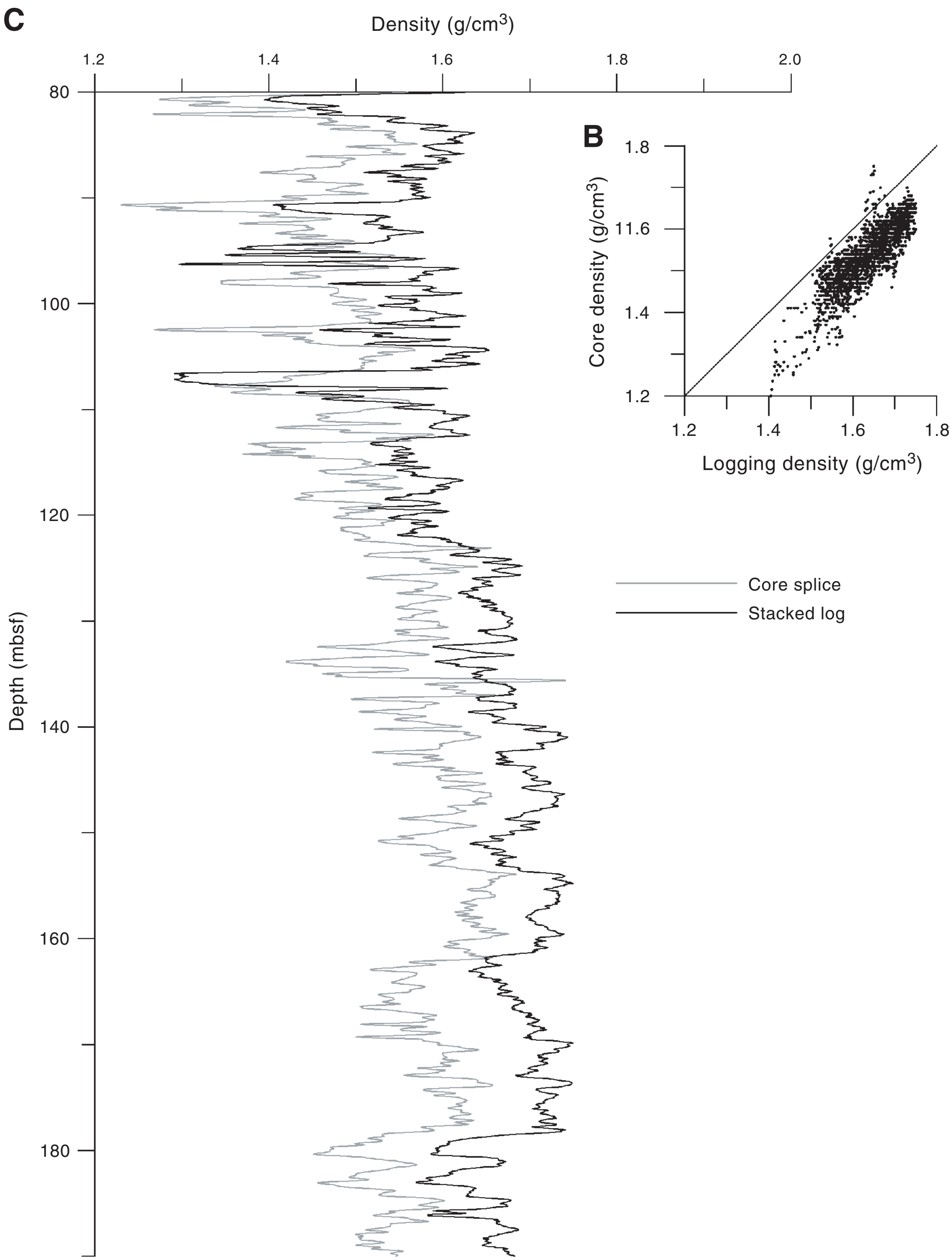

Figure F2. Cross-plot of logging density and corrected (for drilling disturbance and hydraulic rebound) GRA_{hc} density.

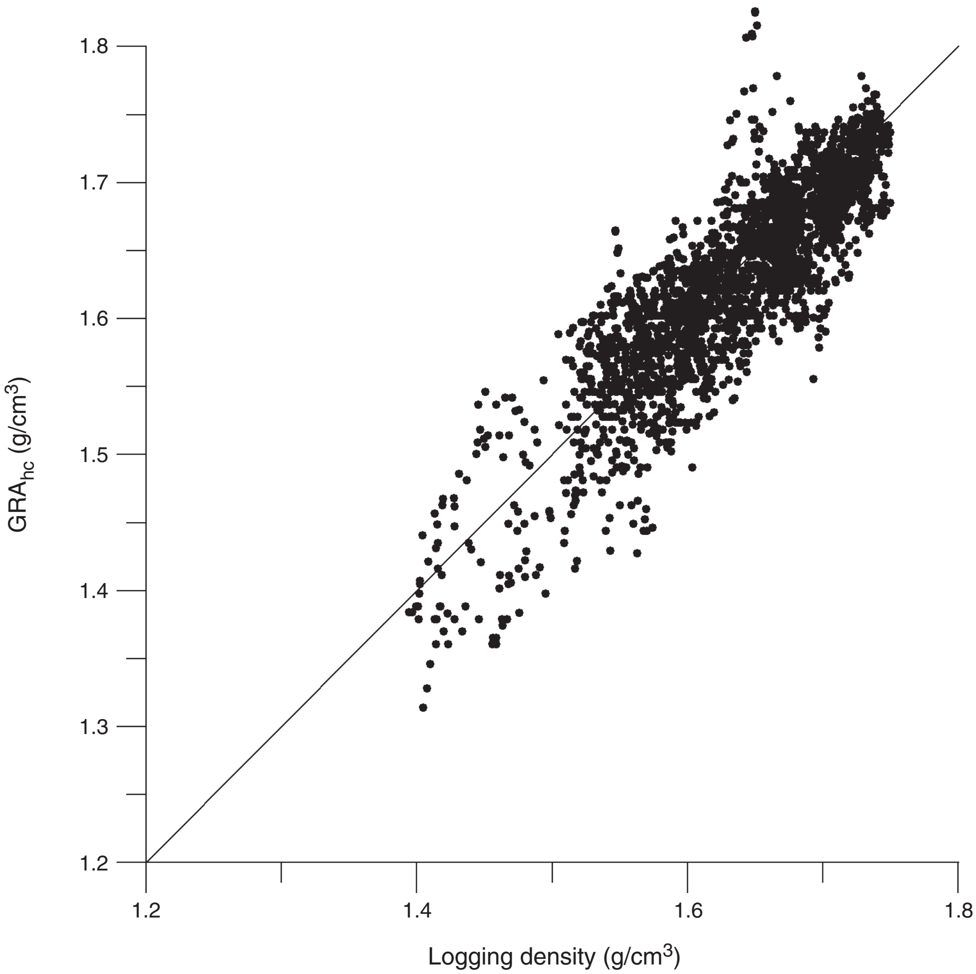

Figure F3. Effective stress (P_i') vs. void ratio (e) relationship for unlithified sediments.

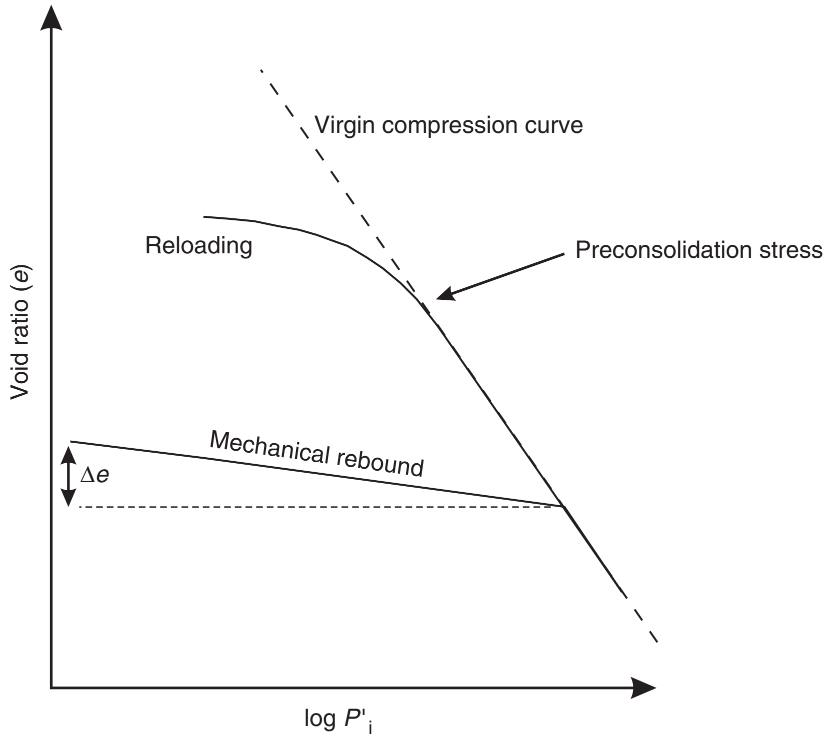

Figure F4. Void ratio (*e*) vs. rebound coefficient (C_r) relationship derived for the nannofossil ooze at Site 1218. Data from other sources were derived from consolidation tests and are shown for comparison.

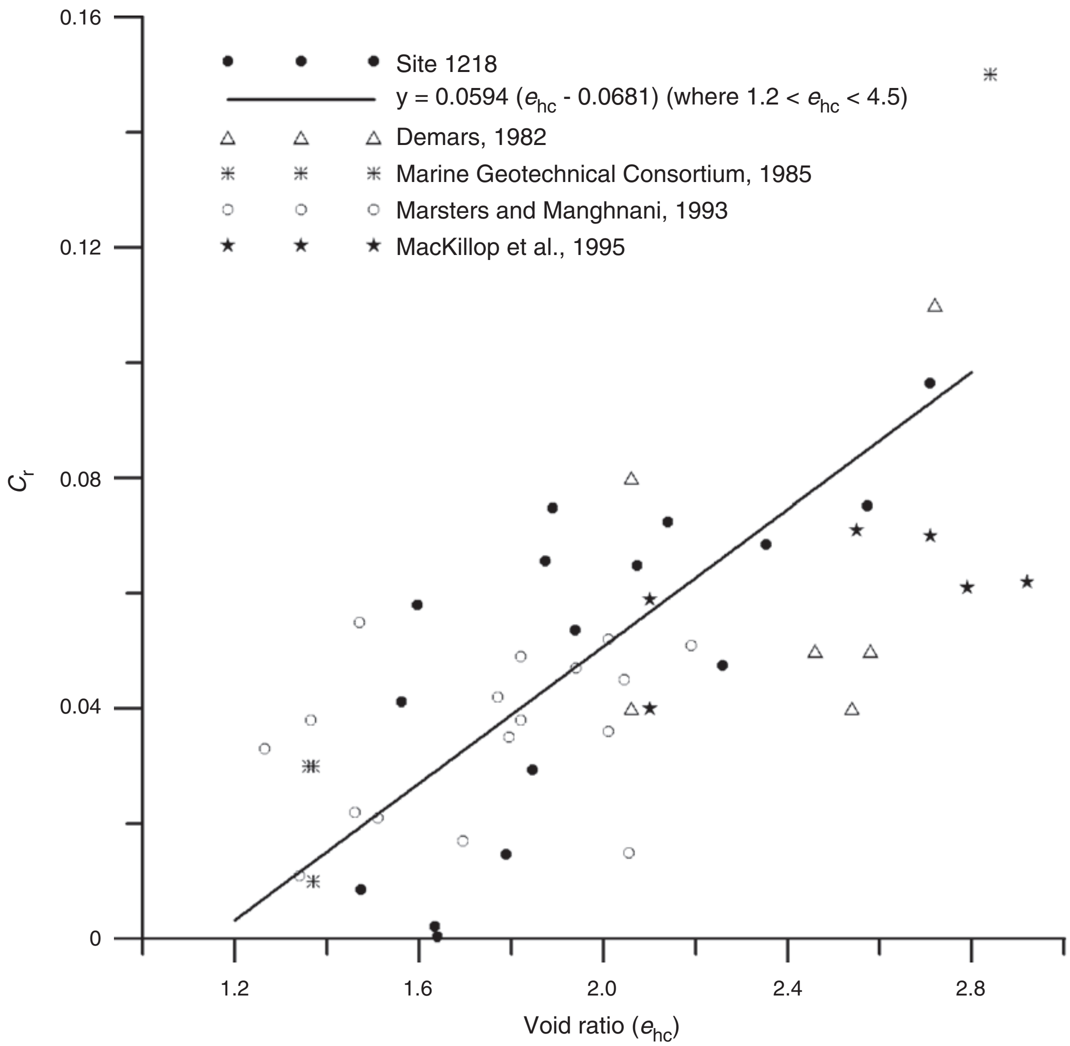

Figure F5. A. Stacked logging density and GRA_{fc}-mcd_{fc} (splice core density corrected for drilling disturbance and hydraulic and mechanical rebound). Note the erroneous logging data from 94.4 to 97.4 mbsf and 106.4 to 110 mbsf. **B.** Depth offset (meters equivalent logging depth [meld; from the Sagan core-log curve match] minus mcd_{fc} [corrected mcd]) between the log and corrected core, plotted in logging mbsf. **C.** Cross-plot of logging density vs. GRA_{fc} (corrected for drilling disturbance and hydraulic and mechanical rebound). It should be noted that erroneous logging data from 94.4 to 97.4 mbsf and 106.4 to 110 mbsf have not been included, although they are plotted in A.

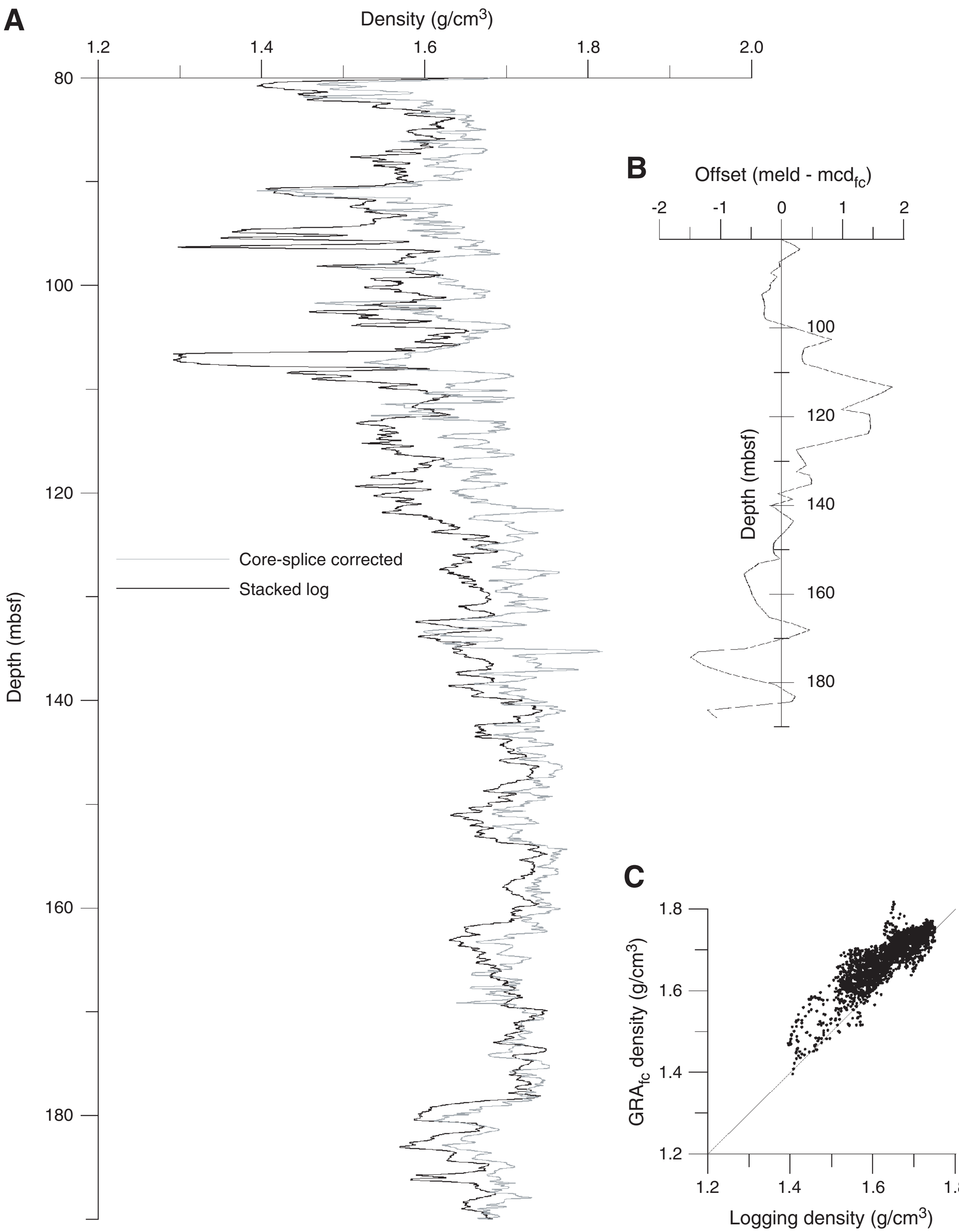

Figure F6. A. GRA_{fc}-mcd_{fc} plotted along with the stacked logging density curve, with the lithofacies shown for reference (Site 1219). The GRA_{fc}-mcd_{fc} is not tied to the logging curve, so the depth match between the two curves is good through the nannofossil ooze. The depth match in the radiolarian ooze is somewhat less satisfactory, and this is interpreted to be the result of erroneous core gaps in the mcd splice. **B.** A cross-plot of depth-matched GRA_{fc}-mcd_{fc} vs. logging density in the radiolarian ooze (Site 1219) indicates a good correction, with the data lying close to the 1:1 (solid) line.

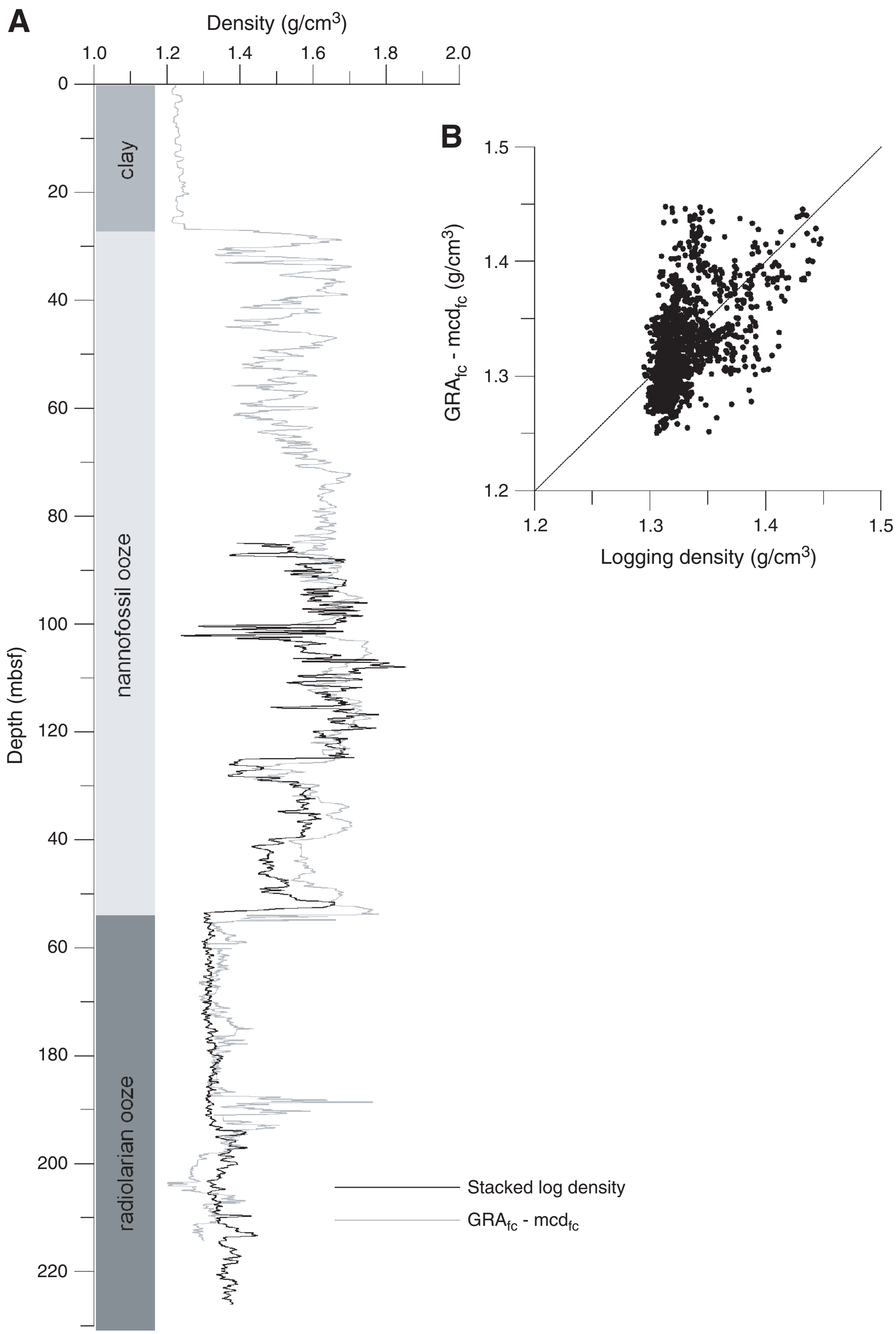

Table T1. List of symbols.

Symbol	Description
$_c$	Corrected for drilling disturbance
cl	Percentage clay content derived from light absorption spectroscopy
C_r	Rebound coefficient
e	Void ratio
$_{fc}$	Final corrected (for coring disturbance, hydraulic, and mechanical rebound)
$_{hc}$	Corrected for drilling disturbance and hydraulic rebound
$_i$	In situ
L	Length
mcd	Meters composite depth
P'_i	Effective in situ pressure
v	Sonic velocity
$_{wi}$	In situ pore water
ΔL	Offset between core mcd and true mbsf depth
ϕ	Porosity
ρ	Density (g/cm^3)

Table T2. In situ water density.

Site	Temperature (°C)	Water depth (mbsl)	Core recovery depth* (mbsf)	In situ water density (kg/m^3)
1215	3.97	5395.6	35	1051.53
1216	3.31	5152.5	25	1050.62
1217	4.62	5342.1	45	1051.20
1218	8.23	4827.6	100	1048.45
1219	8.23	5063.3	100	1049.41
1220	6.59	5217.9	75	1050.35
1221	5.61	5175.3	60	1050.34
1222	3.84	4988.7	33	1049.86

Notes: * = half the depth of APC core recovery. In situ water density was calculated using the water depth, half the depth of APC core recovery, and the geothermal gradient derived from the Advanced Piston Corer Temperature tool measurements.

Table T3. Validity of splice depth corrections to true in situ depths for all sites cored during Leg 199.

Site	Comments
1215	The correction is good to ~50 mcd.
1217	The correction is good to the end.
1218	The correction is good down to 209 mcd, the bottom of Core 199-1218A-20H, where APC ended.
1219	The depth correction is good down to 218.74 mbsf.
1220	The correction is good down to 140.72.
1221	Not corrected.
1222	The correction is good to the end.

Note: Details of the validity of splice depth corrections back to true in situ depths (mcd_{fc}) for all sites cored during Leg 199. The density corrections are good for all unlithified lithologies until advanced piston coring (APC) was terminated.

CHAPTER NOTE*

N1. Rea, B.R., and Gaillot, P., submitted. Calculating sediment rebound coefficients using core-log correlation, for the correction of core physical properties and depths. *Mar. Geol.*

*Dates reflect file corrections or revisions.